# Synthesis and characterization of nanosheet-shaped titanium dioxide

**Mingdeng Wei · Yoshinari Konishi · Hironori Arakawa**

**Abstract** Nanosheet-shaped $TiO_2$ material with a large surface area was synthesized by the reaction of anatase $TiO_2$ with 10 M NaOH aqueous solution at 100 °C for 12–48 h and followed by washing with dilute HCl. Numerous nanosheets were aggregated together and formed a *dahlia* flower. TEM images show that these nanosheets have a rolled edge, suggesting that this material might be an intermediate product in the formation of tubular structural materials. The results of XRD measurement and Laser Raman analysis indicate that the structure of nanosheets is a layered compound, $H_2Ti_3O_7$.

## Introduction

Porous, nanostructured materials have received special attention because of their potential applications in environmental purification, photocatalysts, gas sensors, and photovoltaic cells [1]. Extensive research has been conducted on $TiO_2$ nano materials, such as $TiO_2$ thin films [2], $TiO_2$ nanoparticles [3], and mesoporous $TiO_2$ [4]. In particular, $TiO_2$ nanotubes have larger surface area and higher photocatalytic activity [5]. It has been reported in recent years that $TiO_2$ nanotube can be synthesized using different methods, such as hydrothermal method [6–10], replication process [11], and template technique [5]. Among them, the replication process is not suitable for nanotube powder preparation with smaller diameter due to its dependence on the pore size of the model prepared from porous alumina. Using template technique, the products are required to remove template and have to be calcined at higher temperature, resulting in decrease surface area. Only the hydrothermal method is suitable to prepare nanotube with a smaller diameter (ca. 5 nm) and a thin wall. As well known, small dimensions are very important for the nanostructured materials.

Since the discovery of $TiO_2$ nanotubes prepared by the hydrothermal method [6], most of the further studies have been focused on the formation mechanism [12], the crystal structure [13], and the potential application [13]. Here we describe synthesis and characterization of a new type of nanosheet-shaped $TiO_2$.

M. Wei (✉) · Y. Konishi · H. Arakawa
Photoreaction Control Research Center (PCRC),
National Institute of Advanced Industrial Science
and Technology (AIST), AIST Tsukuba Central #5,
1-1-1, Higashi, Tsukuba, Ibaraki 305-8565, Japan
e-mail: wei-mingdeng@aist.go.jp

*Present Address:*
M. Wei · Y. Konishi
Energy Technology Research Institute, National Institute
of Advanced Industrial Science and Technology (AIST),
AIST Tsukuba Center, Tsukuba, Ibaraki 305-8568, Japan

*Present Address:*
H. Arakawa
Faculty of Engineering, Tokyo University of Science,
Shijiku-ku, Tokyo 162-0826, Japan

## Experimental

### Preparation of nanosheets

In a typical process, 1 g of $TiO_2$ powder (ST-01, obtained from Ishihara Sangyo Kaisha, LTD.) and an

aqueous solution of NaOH (10 M, 200 ml) were placed into a Teflon container. The mixture was vigorously stirred in an oil-bath at 100 °C for 12–48 h. The milk-like suspension was filtrated and washed with dilute HCl and then deionized water until a pH value near 7 was obtained. Finally, the white product was dried at 70 °C for more than 3 h.

Characterization of nanosheets

X-Ray powder diffraction (XRD) patterns were recorded using a diffractometer (Mac Science). Mutil-point BET surface area, pore volume and BJH pore size distribution (PSD) of materials were calculated from the adsorption-desorption isotherm of $N_2$ at 77 K (Micromeritics ASAP 2010). Both scanning electron microscope (SEM) and Transmission electron microscope (TEM) measurements were conducted using a DS-720 (TOPCON Co. Ltd.) and a JEM-2000EXII (JEOL Co. Ltd.), respectively. Laser Raman spectra were measured using a JASCO NRS-1000.

**Results and discussion**

Figure 1a is a low magnification TEM image of a typical product obtained at 100 °C for 12 h showing a *dahlia* flower with ca. 300 nm in diameter. A high magnification image of the edge region of flower revealed that these materials seem to be nanosheets with rolled edge (Fig. 1b). No any tubular structure or raw particle was found. According to the mechanism of formation [12], if the tubular structure were formed, a couple of multi-walls of tube would be observed [8, 13]. As shown in Fig. 1b, these nanosheets are random distribution and have a rolled edge. This structure has not been reported in $TiO_2$ nano materials so far. These results do not in agree with the reports that a large

number of nanotubes were formed for less than 20 h [6, 7, 9, 12, 14, 15]. According to the formation mechanism of $TiO_2$ nanotubes proposed by Wang et al. [12], they considered that the two dimensional lamellar $TiO_2$ is essential for the formation of the $TiO_2$ nanotubes. Therefore, the nanosheets with rolled edge might be an intermediate product. These nanosheets could be converted into tubular structure if the reaction conditions were adjusted.

SEM photographs of nanosheets obtained at different reaction times are shown in Fig. 2. Numerous needle-shaped products are observed and situated close to each other. These needle-shaped products might be a precursor of nanotubes. As shown in Fig. 2a, b, these needle-shaped products have ca. 100–200 nm in length and less than 40 nm in diameter. When the reaction time further increased, the length increased significantly (see Fig. 2c). The image of SEM is very different from that of TEM, only surface state was observed by the former. The needle-shaped might be a edge of nanosheets or a rolled edge of nanosheets.

The $N_2$ adsorption-desorption isotherms of $TiO_2$ nanosheet exhibits an isotherm of type IV with H3 hysteresis and a sharp step at ca. $0.40 < P/P_0 < 0.45$ stage (Fig. 3a). The type H3 loop, which does not exhibit any limiting adsorption at high $P/P_0$, is observed with aggregates of plate-like particles giving rise to slit-shaped pores [16]. This phenomenon causes the artifact in the PSD centered ca. 4 nm (according to the BJH model) and is often referred to as the Tensile Strength Effect (TSE) [17]. Mesoporous with pore necks smaller than 4 nm will release their $N_2$ at a relative pressure of ca. 0.45. Therefore, the amount of $N_2$ desorbing at a relative pressure of ca. 0.45 is real, but it cannot be ascribed to pores of 4 nm diameter alone [18]. Many examples are known where people claim that uniform pores of ca. 4 nm diameter are formed [19–23]. Zhang et al. [14] reported the similar



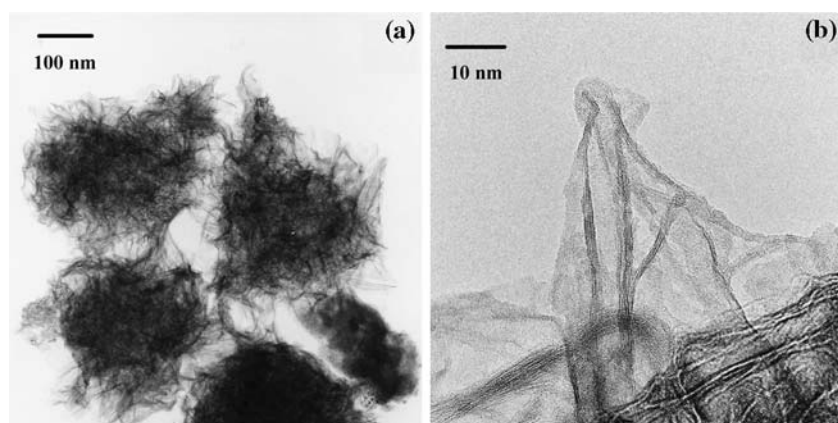**Fig. 1** TEM images of nanosheet (**a**) low magnification, and (**b**) high magnification

**Fig. 2** SEM images of nanosheets at 100 °C for (**a**) 12 h, (**b**) 24 h, and (**c**) 48 h
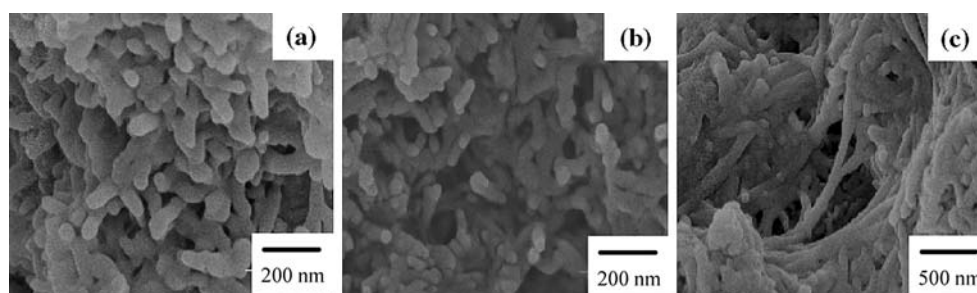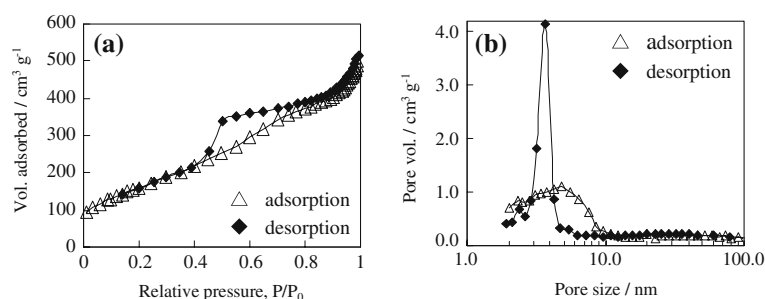


**Fig. 3** $N_2$ adsorption–desorption isotherms (**a**) and pore size distributions (**b**) of nanosheet obtained by the hydrothermal method at 100 °C for 12 h



$N_2$ adsorption-desorption isotherms of $TiO_2$ nanotube. A sharp step at ca. 0.5 stage was also observed and contributed to the characteristic of ordered mesoporous. Obviously, the TSE phenomenon was ignored.

Figure 3b shows PSD of $TiO_2$ nanosheet. No taking into account the TSE phenomenon in the desorption branch PSD would lead to the conclusion that a narrow distribution of pore centered 3.7 nm, while PSD derived from the adsorption branch evidences that the created mesoporous show a broad distribution centered 4.8 nm. Therefore, the peak observed at 3.7 nm cannot be reflected the exact porous properties of the materials, although the intensity of this peak is very high. These pores were formed by a large number of nanosheets. Thus, only the average pore size of desorption branch can be used to express the pore distribution. The nanotubes prepared by the hydrothermal treatment have been confirmed to be hollow pore structure with open end, and their pores size distribution can be determined from the BJH deposition curve. Sun et al. [13] determined the PSD of $TiO_2$ nanotubes and contributed the peak at 3.7 nm to the inner diameter of nanotubes. However, $N_2$ adsorption–desorption isotherms were not given, and the TSE phenomenon cannot be excluded.

The physical properties of $TiO_2$ nanosheets obtained at the different reaction times and the surface area of raw $TiO_2$ (ST-01) are listed in Table 1. It is clear that the surface area of products is larger than that of the raw $TiO_2$. The surface area ($S_{BET}$) of nanosheets tends to decrease with increasing reaction time, while the average pore size increases gradually. This might be attributed to increment of rolled edge of $TiO_2$ nanosheets. It is noted that the PSD calculated from desorption branch (BJH method) unchanged, this is due to appearance of TSE phenomenon. The evidence is that all products show a sharp step at ca. $0.40 < P/P_0 < 0.45$ stage in the desorption branch. Thus, the peak at 3.7 nm cannot be reflected the exact PSD.

The patterns XRD of the raw $TiO_2$ (ST-01) and $TiO_2$ nanosheet are depicted in Fig. 4a, c. The XRD pattern in Fig. 4c shows a typical profile of $TiO_2$ anatase phase, and agrees with the report (JCPDS 21-1272). It is notable that a peak at ca. $2\theta = 10°$ in Fig. 4a was observed for the nanosheets. This is a characteristic of layered compounds [24–26]. According to current structural investigations [27–28], the XRD patterns of nanosheets can be indexed to a layered titanate $H_2Ti_3O_7$ with a monoclinic structure. On the other hand, Sun et al [13] described it as $Na_xH_{2-x}Ti_3O_7$ ($x = 0.75$) according to their EDXA analysis. In this
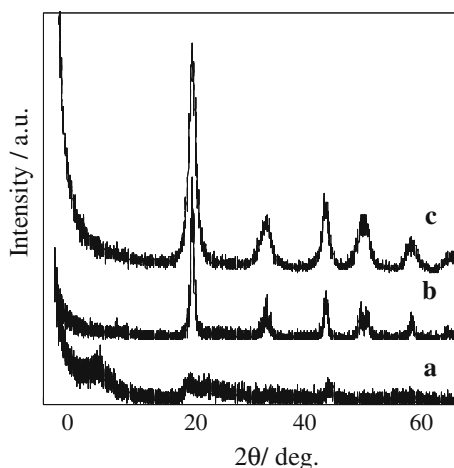
**Table 1** The physical properties of nanosheets at different reaction times

| Reaction Time (h) | $S_{BET}$ ($cm^2g^{-1}$) | Pore volume ($cm^3\ g^{-1}$) | Average pore size* (nm) | Pore size* (nm) |
|---|---|---|---|---|
| Raw $TiO_2$ | 341.2 | — | — | — |
| 12 | 588.9 | 0.756 | 4.4 | 3.7 |
| 24 | 506.9 | 0.698 | 4.7 | 3.7 |
| 48 | 465.1 | 0.672 | 4.9 | 3.7 |

* Calculated from desorption branch

**Fig. 4** XRD patterns of (**a**) nanosheet, (**b**) nanosheet calcined at 525 °C for 2 h, and (**c**) raw $TiO_2$ (ST-01)

study, the product was thoroughly washed with the dilute HCl solution (0.1 M) until a pH value near 7 was reached. ICP analysis shows that the concentration of residual Na ions in the final product is only several ppm. This result also indicates that Na ions in final product cannot be completely removed. Therefore, if the amount of residual Na ions is not calculated, the final product could be described as $H_2Ti_3O_7$. Figure 4b shows the pattern of the nanosheet calcined 525 °C for 2 h in air, it is clear that the phase was converted into anatase $TiO_2$, indicating that the phase of the nanosheet is unstable at higher temperature. This is in agreement with the report by Sun et al. [13]. They investigated the effect of residual Na ions on the thermal stability and found that the thermal stability of product was strongly dependence on the residual Na ions.

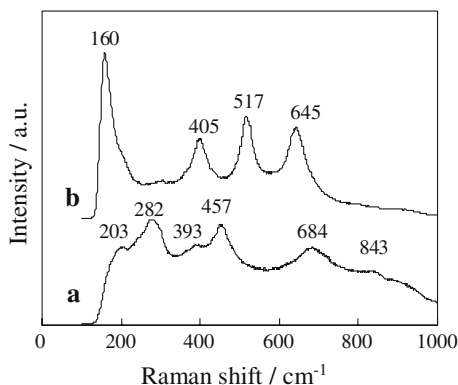Figure 5 shows the laser Raman spectra of the raw $TiO_2$ (ST-01) and $TiO_2$ nanosheet. The peaks at ca.

160, 405, 516, and 645 $cm^{-1}$ in Fig. 5b are due to anatase $TiO_2$ [22]. The peaks of the nanosheet are significantly different from that of the raw $TiO_2$, new peaks at 203, 282, 393, 457, 684, and 843 $cm^{-1}$ were observed, indicating that the phase was varied after reaction. Among them, the peaks at 281 and 684 $cm^{-1}$ were suggested to be due to Ti–O–Na, as reported for $Na_2O–TiO_2$ glass [23]. According to the report [28], $H_2Ti_3O_7$ is composed of $TiO_6$ octahedrons with a edge-sharing, and H atoms are located between the layers. Thus, the residual Na ions are also located between the layers.

## Conclusions

We have successfully synthesizes nanosheet-shaped $TiO_2$ powder with a large surface area. Numerous nanosheets were formed when the raw $TiO_2$ was reacted with NaOH (10 M aqueous solution) at 100 °C for 12–48 h and followed by washing with dilute HCl. These nanosheets were aggregated together and formed a *dahlia* flower with ca. 300 nm in diameter. TEM images show that these nanosheets have a rolled edge, suggesting that this might be an intermediate product in the formation of tubular structural materials. The results of XRD determination and Raman analysis indicate that the structure of nanosheets is a layered compound of $H_2Ti_3O_7$.

## References

1. Bach U, Lupo D, Comte P, Moser JE, Welssörtels F, Scallbeck J, Spreitzer H, Grätezl M (1998) Nature 395: 583
2. Negishi N, Takeuchi K, Ibusuki T (1999) J Mater Sci Lett 18:515
3. Wang C-C, Ying J-Y (1999) Chem Mater 11:3113
4. Yang P-D, Zhao D-Y, Margolese DI, Chmelka BF, Stucky GD (1999) Chem Mater 11:2813
5. Adachi M, Murata Y, Harada M (2000) Chem Lett 8: 942
6. Kasuga T, Hiramatsu M, Hoson A, Sekino T, Niihara K (1998) Langmuir 14:3160
7. Kasuga T., Hiramatsu M., Hoson A., Sekino T, Niihara K (1999) Adv Mater 11:1307
8. Du G-H, Chen Q, Che R-C, Yuan Z-Y, Peng L-M (2001) Appl Phy Lett 79:3702
9. Seo D-S, Lee J-K, Kim H (2001) J Crystal Growth 229:428
10. Ma R-Z, Bando Y, Sasaki T (2003) Chem Phys Lett 380: 577
11. Hoyer P (1996) Langmuir 12:1411
12. Wang Y-Q, Hu G-Q, Duan X-F, Sun H-L, Xue Q-K (2002) Chem Phy Lett 365:427
13. Sun X-M, Li Y-D (2003) Chem Eur J 9:2229
14. Zhang Q-H Gao LS, Zheng S, Sun J (2002) Acta Chimica Sinica 60:1439
15. Zhu Y, Li H, Koltypin Y, Hacohen YR, Gedanken A (2001) Chem Commun 2616

**Fig. 5** Laser Raman spectra of (**a**) nanosheet and (**b**) the raw $TiO_2$ (ST-01)

16. Sing KSW, Everett DH, Haul RAW, Moscou L, Pierotti RA, Rouquérol J, Siemieniewaka T (1985) Pure Appl Chem 57:603
17. Groen JC, Peffer LAA, Pérez-Ramírez J (2003) Micropor Mesopor Mater 60:1
18. Janssen AH, Koster AJ, de Jong KP (2002) J Phy Chem B106:11905
19. Yuan ZY, Wang JZ, Zhang ZL, Chen TH, Li HX (2001) Micropor Mesopor Mater 43:227
20. Keshavaraja A, Ramaswamy V, Soni HS, Ramsawamy AV, Ratnasamy P (1995) J Catal 157:501
21. Colón G, Hidalgo MC, Navío JA (2002) Catal Today 76:91
22. Ocańa M, Garcia-Ramos JV, Serna CJ (1992) J Am Ceram Soc 75:2010
23. Kim HM, Miyaji F, Kokubo T, Nakamura T (1997) J Mater Sci Mater Med 8:341
24. Xu Y-H, Feng Q, Kajiyoshi K, Yanagisawa K (2002) Chem Mater 14:697
25. Xu Y-H, Feng Q, Kajiyoshi K, Yanagisawa K, Yang X-J, Makita Y, Kasaishi S, Ooi K (2002) Chem Mater 14:3844
26. Feng Q, Xu Y-H, Kajiyoshi K, Yanagisawa K (2001) Chem Lett 10:1036
27. Chen Q, Zhou W-Z, Du G-H, Peng L-M (2002) Adv Mater 14:1208
28. Chen Q, Du G-H, Zhou S, Peng L-M (2002) Acta Crystallogr B 58:587